 Bull. Chem. Soc. Jpn. Vol. 80, No. 11, 2137–2144 (2007) 

# Driving Force for a Catalyzed Reaction Derived from a Reaction Rate Spectrum

**Yusuke Yasuda**

Faculty of Science, University of Toyama, Toyama 930-8555

Received March 19, 2007

Based on the acceleration of Gibbs free energy, $-d^2G/dt^2$, a kinetic (or falls) model for a catalyzed CO oxidation was developed. Since $G_T(t)$ of the system inevitably decreases during a reaction, it may be regarded as the height of water in the model; $-d^2G_T/dt^2 \equiv F_T$ corresponding to gravity, may be regarded as the driving force for the reaction to occur. The reaction mechanism for $CO(X) + (1/2)O_2(Y) \rightarrow CO_2(Z)$ can be divided into two parallel transformations, $X \leftrightarrow A_X \leftrightarrow B_X \rightarrow Z_X$ and $Y \leftrightarrow A_Y \leftrightarrow B_Y \rightarrow Z_Y$, which are composed of the three elementary steps accompanied by intermediate A and B. The driving force $F_X$ for $A_X$ and $B_X$ to proceed and also $F_Y$ for $A_Y$ and $B_Y$ were determined separately. Because $F_T$ ($=F_X + F_Y$), $F_X$, and $F_Y$ were independent of $t$ in a definite period, they (instead of $G(t)$) are useful for describing coupling among the elementary steps and correlations among the intermediates. The reaction can be written $X + Y + @ \rightarrow Z^* + @$, where $Z^*$ means that Z leaving catalysts has hyperthermal energy and @ denotes the active site where $B_Y$ (assigned to subsurface oxygen) is located. The present dissipative structure is supported by $F_T$, not by any autocatalytic reaction.

Catalysis is a phenomenon of acceleration of the rate of a chemical reaction by a substance, that is, a catalyst. To find the source of the acceleration is obviously very challenging. Heterogeneous catalytic reactions are in general far from thermodynamic equilibrium, and therefore, one can observe rate oscillations, spatio-temporal patterns, and chaos; a group of phenomena which has been denoted "dissipative structure" by Prigogine and Nicolis.[1] The classical examples of such patterns are traveling waves, target patterns, and rotating spiral waves in the Belousov–Zhabotinsky (BZ) reaction. However, its detailed modeling remains difficult because of the complexity of its reaction scheme and the large number of intermediates products.[2]

Many oscillatory reactions in heterogeneous catalysis have been observed.[3] Usually, all oscillatory reactions are accompanied by spatio-temporal pattern formation, and in order to make these patterns visible, various spatially resolving techniques have been developed.[4]

Catalytic CO oxidation over $Pt/Al_2O_3$ was considered in this work.

$$CO(g)(X) + (1/2)O_2(g)(Y) \rightarrow CO_2(g)(Z). \quad (1)$$

The reaction over platinum group metal surfaces is one of the most extensively studied heterogeneous catalytic reactions due to its practical importance and theoretical interest. This catalytic reaction is able to display the same basic patterns as the BZ reaction.[5]

To describe mathematically these nonlinear dynamics, reaction-diffusion equations of the general form have been applied:

$$\partial c_i/\partial t = F_i(\zeta, \boldsymbol{c}) + D_i \partial^2 c_i/\partial x^2, \quad (2)$$

where $\boldsymbol{c}$ is a vector standing for the concentrations of various chemical species and $\zeta$ denotes a set of parameters. The kinetics of species i are contained in the term $F_i$, whereas diffusion is treated in the usual Laplacian form in the second term with $D_i$ representing the diffusion coefficient.[4] It is worth noting that although material balance is considered in Eq. 2, heat balance in the reaction is not considered and also determining $c_i(x, t)$ from Eq. 2 is in general very difficult, because $F_i(\zeta, \boldsymbol{c})$ is a nonlinear function of $\boldsymbol{c}$ coupled with each other.

On the other hand, according to the second law of thermodynamics, Gibbs free energy ($G$) of a system is decreasing at any moment during a reaction occurring spontaneously under constant pressure and temperature. A reaction such as $X + Y \rightarrow Z$ appears to proceed via a transition state (TS). The TS theory by Eyring[6] and Polanyi and Evans[7] based on $G$ has been a basic theory in the study of reaction kinetics and has been extended to a catalyzed reaction.[8]

Recently, a reaction rate spectroscopy (RRS)[9] available for a catalyzed reaction of gases has been proposed that is schematically shown in Fig. 1a, by which "flow" of Gibbs free energy along the reaction coordinate $\tau$ can be obtained as follows:

$$[-dG/dt]_\tau \equiv J(\tau) \quad (0 < \tau < 1). \quad (3)$$

It should be emphasized that $dG(\tau)/dt$ instead of $G(\tau)$ is considered in RRS as demonstrated in Fig. 1b. Traditional free energy dissipation agrees with $J_T(1)$–$J_T(0)$, whereas $J_T(\tau)$ versus $\tau$ has never been investigated.

According to the RRS, concentration $c_i$ is forced to oscillate harmonically with an angular frequency $\omega$ by varying gas space, instead of controlling dosing rate of a reactant implemented by Ertl et al.;[10] the difference between the two methods is considerable in both experimental and theoretical procedures.[11]

The heterogeneity of concentration over catalysts corresponding to the term of $D_i \partial^2 c_i/\partial x^2$ is forced to oscillate. Fre-

Published on the web November 13, 2007; doi:10.1246/bcsj.80.2137

quency response of the system to the perturbation depends on $F_i(\zeta, \Delta \boldsymbol{c})$ as well as $D_i$. Remarkable merits of RRS are that both material and heat balances can be considered via $dG/dt$ as shown below and further that any function, such as $F_i(\zeta, \Delta \boldsymbol{c})$, can be linearized by a Taylor series expansion, because perturbation $\Delta \boldsymbol{c}$ is very small. The left hand side of Eq. 2 can be expressed by $i\omega\Delta c_i$, because the variation $\Delta c_i(t)$ is harmonic. Simultaneous linear equations of $\Delta \boldsymbol{c}$ thus derived can be analytically solved.

The reaction mechanism adopted in this work is shown in Fig. 2, which is composed of the three elementary steps, I, II, and III, accompanied by two intermediates, A and B. The reaction is divided into two parallel transformations, (i) and (ii). Whether $A_Y$ is associatively or dissociatively adsorbed did not affect RRS data analysis carried out below.

In this work, $J(\tau)$ determined previously[9] was translated to a definite function of time, $J(t)$. Then, integration of $J(t)$ led to $G(t)$, whereas the time derivative $dJ(t)/dt$ yielded a force $F$ for the reaction to occur. The study of reaction kinetics based on $F$ (instead of $G(t)$) is shown to be effective to describe coupling among the elementary steps and correlations among the intermediates. The source of $F$ is also discussed.

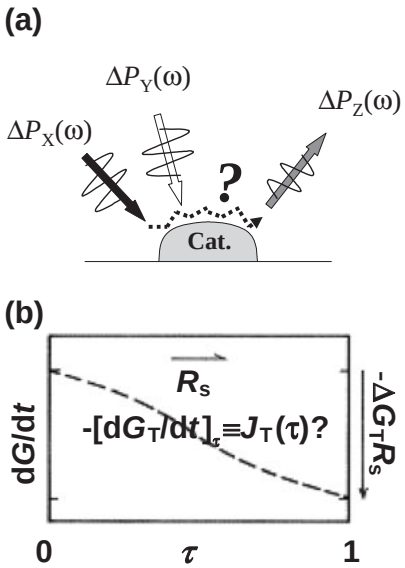


Fig. 1. (a) Basic idea of RRS for a reaction of $X + Y \rightarrow Z$. (b) "Flow" of Gibbs free energy, $J_T(\tau) \equiv -[dG_T/dt]_\tau$, obtainable by RRS vs. the reaction coordinate $\tau$. ($R_s$) the rate of reaction in steady state; ($-\Delta G_T$) the free energy fall in the reaction. The difference $J_T(1) - J_T(0)$ corresponds to free energy dissipation in the reaction ($=-\Delta G_T R_s$), while $J_T(\tau)$ vs. $\tau$ has never been investigated.

## RRS

**Experimental.** In RRS, a part of gas space, $\Delta V(\omega; t)$ ($10^{-2}$ of a constant-flow reactor at steady-state), was varied harmonically over a wide range of angular frequency $\omega$ ($5 \times 10^{-3}$–$3 \times 10^{-1}$ Hz). Frequency response of the system to $\Delta V(\omega; t)$ was observed by following pressure variation $\Delta P_W(\omega; t)$ (W = X, Y, and Z).

The spectrum was characterized by using complex rate coefficient $k^*$ defined by $(k + i\omega l)$.[9] The sixteen rate coefficients, $k$ and $l$, contained in the reaction mechanism were determined by numerical simulation of the spectrum. They are summarized in Table 1.

Since every reaction rate is expected to be proportional to the amount of active site $N_a$, $J(\tau)$ was divided by $N_a$ in order to make it characteristic for catalysts:

$$j(\tau) \equiv J(\tau)/N_a \equiv [-dg(\tau)/dt]_\tau. \quad (4)$$

It is noted that the parameters in Table 1 are independent of amounts of catalysts and therefore characteristic for catalysts.

**Results of $\delta j$'s.** The function $j(\tau)$ is composed of several parts, $\{\delta j(\tau_n)\}$:

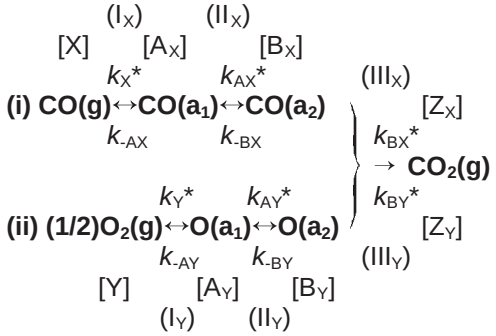


Fig. 2. Reaction mechanism for a CO oxidation reaction ($X + Y \rightarrow Z$) composed of the three elementary steps, I, II, and III, accompanied by two intermediates, A and B; $A_Y$ may be either associatively or dissociatively adsorbed. The whole reaction is divided into two parallel transformations, (i) $X \leftrightarrow A_X \leftrightarrow B_X \rightarrow Z_X$ and (ii) $Y \leftrightarrow A_Y \leftrightarrow B_Y \rightarrow Z_Y$. Frequency response of every forward reaction to harmonic oscillation of $\Delta P_X(t)$ and $\Delta P_Y(t)$ is characterized by the complex rate coefficient $k^* \equiv k + i\omega l$, whereas the response to every reverse reaction is characterized by real $k$.

Table 1. Rate Coefficient[a)] of the Reaction Mechanism Shown in Fig. 2 (Units of $k$: $min^{-1}$)

| $k_X$ | $l_X$ | $k_{-AX}$ | $k_{AX}$ | $l_{AX}$ | $k_{-BX}$ | $k_{BX}$ | $l_{BX}$ |
|---|---|---|---|---|---|---|---|
| −1.512 | −0.52 | 28.1 | 15.4 | (−0.333)[b)] | 294 | 81.2 | 0.904 |
| $k_Y$ | $l_Y$ | $k_{-AY}$ | $k_{AY}$ | $l_{AY}$ | $k_{-BY}$ | $k_{BY}$ | $l_{BY}$ |
| −0.73 | −0.582 | 1.15 | 0.435 | (−0.5) | −0.074 | 0.28 | (−0.5) |

a) Experimental conditions: $P_X^{(s)} = 116$, $P_Y^{(s)} = 86$, $P_Z^{(s)} = 72$ Pa over $Pt/Al_2O_3$ at 623 K. b) The value in the parenthesis is fixed (see text).

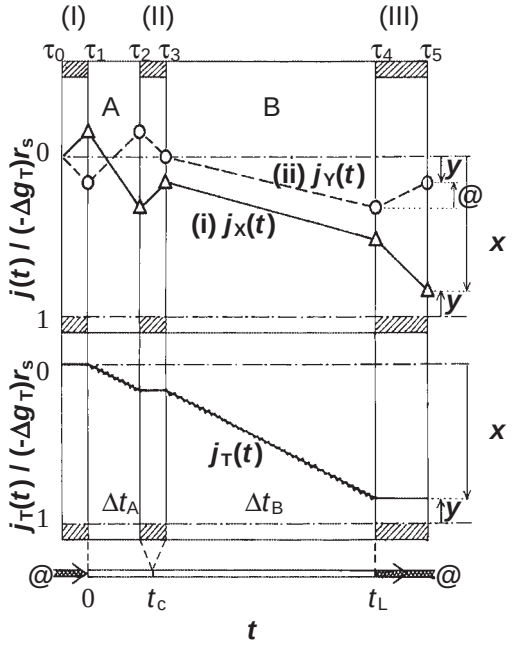


Fig. 3. Results of various $j(t) = -[\mathrm{d}g/\mathrm{d}t]_t$ determined by RRS vs. time. The variations along (i) and (ii) in Fig. 2 are shown by $j_X(t)$ and $j_Y(t)$, respectively; $j_T(t)$ is the sum of $j_X(t) + j_Y(t)$.

$$\delta j(\tau_n) \equiv j(\tau_n) - j(\tau_{n-1}) \quad (n = 1\text{–}5). \tag{5}$$

Notation of $\tau_0$–$\tau_5$ is illustrated in Fig. 3; although every $\tau_n$ is indicated separately, $\tau_0$ and $\tau_1$ in step I (and $\tau_2$ and $\tau_3$ concerning step II) overlaps, because disappearance of X and appearance of $A_X$ at step $I_X$, for example, is assumed to occur instantaneously. Free energy dissipations, on the other hand, occur in the periods between $\tau_1$ and $\tau_2$ via A species and also between $\tau_3$ and $\tau_4$ via B species.

In the numerical simulation to determine the rate coefficients on a trial and error basis, two relations have been derived:[9]

$$l_{AX} = -1/3 \text{ and } l_{AY} + l_{BY} = -1. \tag{6}$$

(1) When $l_{AX} = -1/3$, the general formulas, $\{\delta J_X(\tau_n)\}$, derived previously[9] are reduced to

$$\begin{aligned}
\delta j_X(\tau_1) &= -(l_{BX}/L_X)x(-\Delta g_T)r_s;\\
\delta j_X(\tau_2) &= 3(l_{BX}/L_X)x(-\Delta g_T)r_s;\\
\delta j_X(\tau_3) &= -(l_{BX}/L_X)x(-\Delta g_T)r_s;\\
\delta j_X(\tau_4) &= (2/L_X)x(-\Delta g_T)r_s;\\
\delta j_X(\tau_5) &= 2(l_{BX}/L_X)x(-\Delta g_T)r_s,
\end{aligned} \tag{7}$$

where $L_X \equiv 2 + 3l_{BX}$ and $r_s \equiv R_s/N_a$ (named turnover frequency); the free energy fall $(-\Delta g_T)$ may be evaluated from the chemical potentials by

$$-\Delta g_T \equiv \mu(\mathrm{CO(g)}) + (1/2)\mu(\mathrm{O_2(g)}) - \mu(\mathrm{CO_2(g)}), \tag{8}$$

which was 229.2 kJ under the experimental conditions (see Table 1).

(2) We adopted $l_{BY} = -1/2$ in this work (and then $l_{AY} = -1/2$), instead of the value of $-0.505$ determined previously[9] (the deviation from $-1/2$ will be discussed below). Then, the general formulas, $\{\delta J_Y(\tau_n)\}$, derived previously[9] reduced to

$$\begin{aligned}
\delta j_Y(\tau_1) &= y(-\Delta g_T)r_s;\\
\delta j_Y(\tau_2) &= -2y(-\Delta g_T)r_s;\\
\delta j_Y(\tau_3) &= y(-\Delta g_T)r_s;\\
\delta j_Y(\tau_4) &= 2y(-\Delta g_T)r_s;\\
\delta j_Y(\tau_5) &= -y(-\Delta g_T)r_s.
\end{aligned} \tag{9}$$

The values of $x(-\Delta g_T)$ and $y(-\Delta g_T)$ in Eqs. 7 and 9 mean the free energy falls in the course of (i) and (ii), respectively.

(3) Since both step I and II are assumed to occur instantaneously (like a collision), the total free energy change at each step would vanish (in analogy with momentum conservation at the collision):

$$\delta j_X(\tau_1) + \delta j_Y(\tau_1) = 0 \tag{10}$$

$$\delta j_X(\tau_3) + \delta j_Y(\tau_3) = 0 \tag{11}$$

These relations combined with $x + y = 1$ lead to

$$x = (2 + 3l_{BX})/(2 + 4l_{BX});\ y = l_{BX}/(2 + 4l_{BX}). \tag{12}$$

(4) From Eq. 7,

$$\delta j_X(\tau_2) + \delta j_X(\tau_4) = x(-\Delta g_T)r_s, \tag{13}$$

which means that the sum of free energy dissipations via $A_X$ and $B_X$ is constant irrespective of the value of $l_{BX}$. On the other hand, Eq. 9 lead to

$$\delta j_Y(\tau_2) + \delta j_Y(\tau_4) = 0, \tag{14}$$

which means that the dissipations via $A_Y$ and $B_Y$ are cancelled out in the course of the reaction.

**Formulas of *j*'s.** The formula of $j_X(\tau_n)$ (or $j_Y(\tau_n)$) is given by the sum of $\delta j$'s in Eq. 7 (or Eq. 9):

$$j_X(\tau_n) = \sum_{m=1}^{n} \delta j_X(\tau_m);\ j_Y(\tau_n) = \sum_{m=1}^{n} \delta j_Y(\tau_m), \tag{15}$$

provided that $j_X(\tau_0) = j_Y(\tau_0) = 0$.

(1) At first, the sum of them

$$j_T(\tau_n) \equiv j_X(\tau_n) + j_Y(\tau_n), \tag{16}$$

is considered.

Substituting Eqs. 7 and 9 into Eq. 16 and considering $x$ and $y$ in Eq. 12, we obtain[9]

$$j_T(\tau_2) = y(-\Delta g_T)r_s, \tag{17}$$

and

$$j_T(\tau_4) = x(-\Delta g_T)r_s. \tag{18}$$

Here, a falls model is introduced: it was assumed that $j_T(\tau_n)$ can be expressed by a linear function of $t$ describing an uniformly accelerated motion (in analogy with gravity) as shown in Fig. 3:

$$j_T(t) = f_T t;\ f_T = x(-\Delta g_T)r_s/t_L \quad (0 < t < t_L), \tag{19}$$

where $t_L$ means the elapsed time of reaction. According to the falls model (i) the free energy $g_T(t)$ corresponds to the height of water at a time, (ii) the time derivative $-\mathrm{d}g_T(t)/\mathrm{d}t \equiv j_T(t)$ corresponds to the change in the falling speed, and (iii) the acceleration of $-\mathrm{d}^2g_T(t)/\mathrm{d}t^2 = \mathrm{d}j_T(t)/\mathrm{d}t \equiv f_T$ corresponds to the acceleration of gravity.

If $l_{BX} = 0.904$ (see Table 1) is accepted, Eq. 12 leads to

$$x = 0.839 \text{ (or } y = 0.161). \tag{20}$$

The boundary between species A and B is given by $(y/x)t_L$ or $0.192t_L$ which is indicated by $t_c$ in Fig. 3; $\Delta t_A \equiv t_c$ and $\Delta t_B \equiv t_L - t_c$ are introduced for convenience.

(2) Both $j_X(t)$ and $j_Y(t)$ are shown together versus $t$ in Fig. 3, of which components, $\{\delta J_X(\tau_n)\}$ and $\{\delta J_Y(\tau_n)\}$, are indicated by the triangles and circles, respectively. Their explicit formulas are expressed as follows:

(a) In the period of $\Delta t_A$ ($\tau_1 \leqq \tau \leqq \tau_2$), we have

$$j_X(t) = \delta j_X(\tau_1) + f_{AX}t;\ f_{AX} = \delta j_X(\tau_2)/\Delta t_A. \tag{21}$$

Substituting the parameters in Table 1 into $\delta j_X(\tau_1)$ and $\delta j_X(\tau_2)$ given in Eq. 7 affords

$$\begin{aligned} j_X(t) &= \eta\{-1 + (3/0.192)(t/t_L)\}(-\Delta g_T)r_s, \\ &\equiv j_{AX}(t) \end{aligned} \tag{22}$$

where

$$\eta = -\delta j_X(\tau_1)/\{(-\Delta g_T)r_s\}. \tag{23}$$

Similarly, we have

$$j_Y(t) = \delta j_Y(\tau_1) + f_{AY}t;\ f_{AY} = \delta j_Y(\tau_2)/\Delta t_A. \tag{24}$$

Substituting the parameters in Table 1 into $\delta j_Y(\tau_1)$ and $\delta j_Y(\tau_2)$ given in Eq. 9 gives

$$\begin{aligned} j_Y(t) &= \eta\{1 - (2/0.192)(t/t_L)\}(-\Delta g_T)r_s \\ &\equiv j_{AY}(t), \end{aligned} \tag{25}$$

where

$$\eta = \delta j_Y(\tau_1)/\{(-\Delta g_T)r_s\}\ (=y). \tag{26}$$

(b) In the period of $\Delta t_B$ ($\tau_3 \leqq \tau \leqq \tau_4$), in a similar way to $\Delta t_A$,

$$j_X(t) = j_X(\tau_3) + f_{BX}t;\ f_{BX} = \delta j_X(\tau_4)/\Delta t_B, \tag{27}$$

and

$$j_Y(t) = j_Y(\tau_3) + f_{BY}t;\ f_{BY} = \delta j_Y(\tau_4)/\Delta t_B, \tag{28}$$

which lead to

$$\begin{aligned} j_X(t) &= [\{\eta - 0.441(t_c/t_L)\} + 0.441(t/t_L)](-\Delta g_T)r_s \\ &\equiv j_{BX}(t), \end{aligned} \tag{29}$$

and

$$\begin{aligned} j_Y(t) &= 2.48\eta\{-(t_c/t_L) + (t/t_L)\}(-\Delta g_T)r_s \\ &\equiv j_{BY}(t). \end{aligned} \tag{30}$$

The results for various $f$'s determined above are shown versus $t$ in Fig. 4.

(c) The changes in $-\delta j_X(\tau_1)$ and $\delta j_Y(\tau_1)$ at step I occur instantaneously. Therefore, they may be regarded as "impulse" or momentum change at the collision between X and Y species; the results are valid also at step II. The impulse is demonstrated by the triangle in Fig. 4, where $\eta$ is defined by

$$\begin{aligned} -\delta j_X(\tau_1)/\{(-\Delta g_T)r_s\} &= \delta j_Y(\tau_1)/\{(-\Delta g_T)r_s\} \\ &= -\delta j_X(\tau_3)/\{(-\Delta g_T)r_s\} \\ &= \delta j_Y(\tau_3)/\{(-\Delta g_T)r_s\} = \eta. \end{aligned} \tag{31}$$

**Regeneration of Active Site.** (1) Because step III was assumed to occur instantaneously, we have a restriction similar to Eqs. 10 and 11:

$$\delta j_X(\tau_5) + \delta j_Y(\tau_5) = y(-\Delta g_T)r_s, \tag{32}$$

which is illustrated in Fig. 3; it seems that $y(-\Delta g_T)r_s$ corresponds to the power produced in the reaction for Z leaving a surface.

By analysis of time-of-flight spectrum[12] or IR-emission spectrum,[13] it has been found that a $CO_2$ molecule leaving a platinum surface has excess translational, rotational, and vibrational energies. The hyperthermal energy corresponds to $y(-\Delta g_T)$ indicated in Fig. 3. The value of $y(-\Delta g_T)$ was 36.90 kJ ($=4440\,\text{K} \times k$) in this work, which is comparable to the sum of those obtained by the two kinds of spectrum analysis.

Substituting the relation of $\delta j_X(\tau_5) = -2\delta j_X(\tau_1)$ given in Eqs. 7 into Eq. 32 gives

$$\delta j_Y(\tau_5) = -y(-\Delta g_T)r_s, \tag{33}$$

where $\eta$ is replaced by $y$. Because $\delta j_Y(\tau_5)$ can be regarded as the power required to regenerate the active site as shown by @ in Fig. 3, the reaction can be written as

$$X + Y + @ \rightarrow Z^* + @ \tag{34}$$

where $Z^*$ means that the product Z leaving catalysts has the hyperthermal energy. Since the power for @ is always accompanied by the power of $y(-\Delta g_T)r_s$ for $Z_Y$ (see Fig. 2), @ is assigned to the site where $B_Y$ is located.

Since Gibbs free energy must decrease at any moment, transition $Y \rightarrow A_Y$ at step I (see Fig. 3), for example, would play an active role, whereas transition $X \rightarrow A_X$ plays a passive role in the collision. In a similar way, the transition $A_Y \rightarrow B_Y$ at step II and also $B_X \rightarrow Z_X$ at step III are expected to play active roles, whereas the other transitions of $A_X \rightarrow B_X$ and

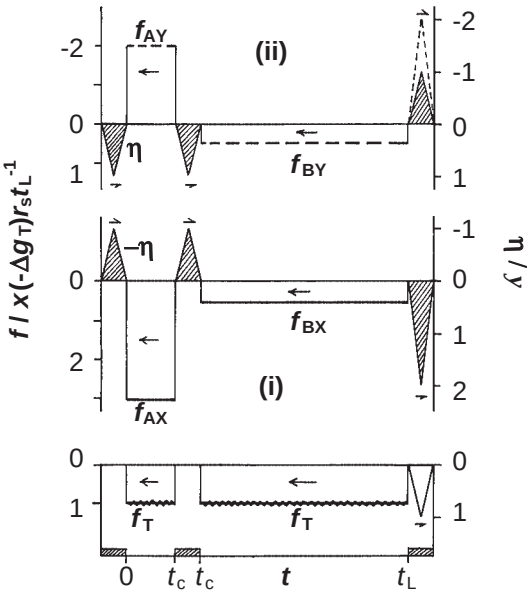


Fig. 4. Driving force $f$ vs. $t$; $f$ is given by $dj(t)/dt$ from $j(t)$ shown in Fig. 3, i.e., $f = dj(t)/dt$; $f_T = f_A + f_B$. The triangle represents "impulse" at step I, II, or III due to the collision between the species belonging to (i) and (ii).

$B_Y \rightarrow Z_Y$ play passive roles. Consequently, it is concluded that half of the impulse due to $B_X \rightarrow Z_X$ is spent for the regeneration of active site (=@$(-\Delta g_T)r_s$) and the other half is spent for the production of excited molecule (=$y(-\Delta g_T)r_s$); if $l_{BY} \leq -1/2$ has been adopted in above section, we would have the result of $y \leq$ @.

**Change in Height.** (1) Integration of the linear function of $j_T(t)$ given in Eq. 19 yields

$$g_T(t) = -(1/2)f_T t^2, \tag{35}$$

provided that $g_T(0) = 0$. On the other hand, according to Eq. 18, the value of $g_T(t_L)$ is expected to be given by (see Fig. 5)

$$g_T(t_L) = -x(-\Delta g_T). \tag{36}$$

Comparing Eqs. 35 and 36, we have

$$f_T = 2x(-\Delta g_T)/{t_L}^2. \tag{37}$$

The different expressions for $f_T$ given in Eqs. 19 and 37 lead to

$$r_s = 2/t_L. \tag{38}$$

(2) Integration of $j_{AX}(t)$ and $j_{AY}(t)$ in Eqs. 22 and 25 leads to the change in height, respectively:

$$g_{AX}(t) = \eta\{2(t/t_L) - (3/0.192)(t/t_L)^2\}(-\Delta g_T), \tag{39}$$

and

$$g_{AY}(t) = 2\eta\{-(t/t_L) + (1/0.192)(t/t_L)^2\}(-\Delta g_T), \tag{40}$$

where $r_s$ is replaced by $2/t_L$.

In a similar way, the integration of Eqs. 29 and 30 leads to

$$g_{BX}(t) = \{0.0146 - 0.1528(t/t_L) - 0.4405(t/t_L)^2\}(-\Delta g_T), \tag{41}$$

and

$$g_{BY}(t) = [-0.0146 + 0.95\eta(t/t_L) - 2.475\eta(t/t_L)^2](-\Delta g_T). \tag{42}$$

Here, the integral constants for $g_{AX}(t)$ and $g_{BX}(t)$ and also those for $g_{AY}(t)$ and $g_{BY}(t)$ were chosen so as to be continuous at step I and II, i.e.,

$$g_{AX}(0) = g_{AY}(0) = 0; g_{AX}(t_c) = g_{BX}(t_c); g_{AY}(t_c) = g_{BY}(t_c). \tag{43}$$

These functions as well as $g_T(t)$ are shown together in Fig. 5. It is noted that the difference between the gradients on both sides of $t = 0$ (at step I) and also those on both sides of $t = t_c$ (at step II) are proportional to $\eta$ so that every gradient is not continuous at the boundaries of step I and II.

It should be emphasized that $g(t)$ and $f$ are correlated with each other by $d^2g(t)/dt^2 = -f$ and both of them are characterized by the same number of the kinetic parameters. However, $g(t)$ appears more complicated than $f$ as compared in Figs. 4 and 5 so that $f$ would be effective rather than $g(t)$ to describe coupling among the elementary steps and relations among the intermediates.

Every $g(t)$ is a parabolic orbital. The unusual orbital of $g_{AY}(t)$ arises from the negative $f_{AY}$, which arises from the correlation of $f_{AX} + (-f_{AY}) = f_T$ (>0) (see Fig. 3 or 4). It seems of interest that "enthalpy unfavorable process" is found in CO adsorption on O-saturated Ag/Pt(110) composite surface, i.e., the surface species may migrate from strongly bound sites to weakly bound sites.[14]

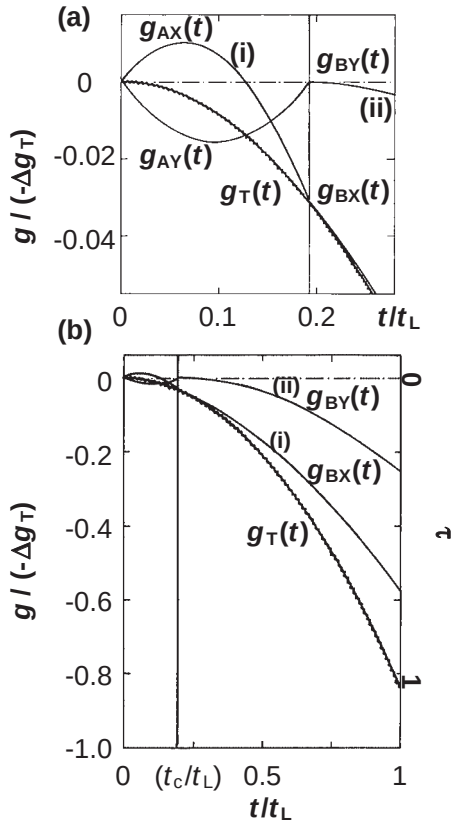


Fig. 5. (a) Gibbs free energy $g(t)$ vs. the reduced time $t/t_L$ in (i) and (ii); the gradient $-dg(t)/dt$ of each curve agrees with $j(t)$ shown in Fig. 3. (b) Those over the whole range of reaction; $g_T(t) = g_A(t) + g_B(t)$. The reaction coordinate $\tau$ proportional to $g_T(t)$ is demonstrated.

## Rate Oscillation

**$ds_T^{univ}/dt$ Due to $j_T(t)$.** In a non-equilibrium system, the catalyst temperature $T_{cat}$ is different from that of thermal surroundings, $T_{therm}$. The rate of entropy of universe, $ds_T^{univ}/dt$, can be expressed by[9]

$$ds_T^{univ}/dt = \{x(-\Delta g_T) + \delta T(\Delta s_T)\}r_s/T_{therm}, \tag{44}$$

where

$$T_{therm} \equiv T_{cat} + \delta T, \tag{45}$$

and $\Delta s_T$ denotes the entropy fall defined by

$$-\Delta s_T \equiv s(CO(g)) + (1/2)s(O_2(g)) - s(CO_2(g)). \tag{46}$$

Because the condition of $|\delta T| \ll T_{therm}$ is satisfied in this work,

$$ds_T^{univ}/dt = x(-\Delta g_T)r_s/T_{therm}, \tag{47}$$

which can be rewritten using Eq. 19 as

$$ds_T^{univ}(t_L)/dt = j_T(t_L))/T_{therm}. \tag{48}$$

**$ds_T^{univ}/dt$ Due to Heat Flow.** The heat of reaction may be expressed by

$$-\Delta h_T \equiv h(CO(g)) + (1/2)h(O_2(g)) - h(CO_2(g)), \tag{49}$$

in terms of the molar enthalpy $h$ of each component; $-\Delta h_T$ was 283.6 kJ at 623 K (see Table 1).[15]

The reaction coordinate $\tau$ adopted in Eq. 3 can be translated to $t$ by the function of

$$\tau(t) = (1/2)\alpha_T t^2, \tag{50}$$

which is proportional to $g_T(t)$ as indicated in Fig. 5. If $\tau(t_L) = 1$, then

$$\alpha_T = 2/{t_L}^2. \tag{51}$$

The heat of reaction generated in the course of reaction, $q_+(t)$, may be expressed by

$$q_+(t) = (-\Delta h_T)(d\tau/dt) = (-\Delta h_T)\alpha_T t. \tag{52}$$

On the other hand, outflow of the heat from catalysts to thermal surroundings, $q_-(t)$, may be expressed by

$$q_-(t) = \lambda(T_{cat} - T_{therm}), \tag{53}$$

where $\lambda$ denotes the thermal conductivity.

Heat balance of $q_+(t) = q_-(t)$ has to be maintained throughout the reaction in the steady state and thus

$$T_{cat} - T_{therm} = \{(-\Delta h_T)\alpha_T/\lambda\}t, \tag{54}$$

which means that the difference between $T_{cat}$ and $T_{therm}$ increases with an increase in $t$. Actually, temperature variations of several tens of degrees during rate oscillations on a supported Pt catalysts have been observed.[16]

On the other hand, the rate $ds_T{}^{univ}(t)/dt$ due to $q_-(t)$ may be expressed by

$$ds_T{}^{univ}(t)/dt = q_-(t)(-1/T_{cat} + 1/T_{therm}) \tag{55}$$

Considering Eqs. 52–54 in Eq. 55, we have

$$ds_T{}^{univ}(t)/dt = \{(-\Delta h_T)^2{\alpha_T}^2/(\lambda T_{cat}T_{therm})\}t^2. \tag{56}$$

**Source of $f_T$.** The function $ds_T{}^{univ}(t)/dt$ in Eq. 56 has to agree with Eq. 48 at $t = t_L$ and thus

$$(-\Delta h_T)^2{\alpha_T}^2{t_L}^2/\lambda T_{cat} = x(-\Delta g_T)r_s. \tag{57}$$

Substituting $\alpha_T$ in Eq. 51 and $r_s$ in Eq. 38 into Eq. 57, we can derive the final expression for $t_L$:

$$1/t_L = (1/2)\lambda T_{cat}x(-\Delta g_T)/(-\Delta h_T)^2 \tag{58}$$

such that

$$r_s = 2/t_L = \lambda T_{cat}x(-\Delta g_T)/(-\Delta h_T)^2. \tag{59}$$

Substituting Eqs. 58 and 59 into $f_T$ given in Eq. 19 gives

$$f_T = (1/2)(\lambda T_{cat})^2\{x(-\Delta g_T)\}^3/(-\Delta h_T)^4. \tag{60}$$

It is worth noting that $\lambda$ plays an important role in $r_s$ and $f_T$, especially since $r_s$ is proportional to $\lambda$.

**Origin of Rate Oscillation.** Although rate oscillation was not observed in this work, oscillatory behavior for CO oxidation has often been observed.[4,5] The origin of oscillation may be explained as follows: (1) The heat of reaction $q_+(t)$ increases linearly with $t$ while $ds_T{}^{univ}(t)/dt$ due to $q_-(t)$ increases with $t^2$ as expressed in Eq. 56. Therefore, the heat balance of $q_+(t) = q_-(t)$ would be broken at $t_L$. (2) Equation 56 means that $s_T{}^{univ}(t)$ is proportional to $t^3$, of which behavior is demonstrated in Fig. 6. The period of the oscillation would be longer

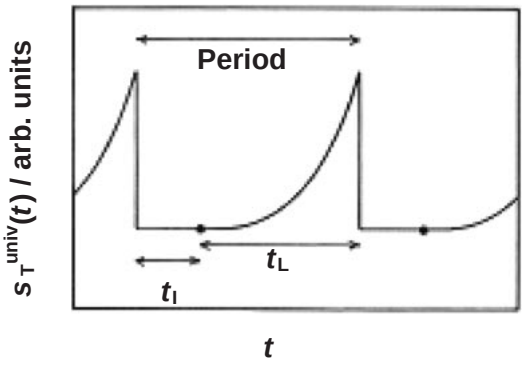


Fig. 6. Periodic oscillation of $s_T{}^{univ}(t)$ vs. $t$. ($t_I$) induction period; ($t_L$) elapsed time for the reaction.

than $t_L$, because the induction period $t_I$ is positive in general;[17] synchronization among active site $N_a$ would proceed during the period. It should be emphasized that the entropy of universe, a measure of deviation from an equilibrium state, increases acceleratedly with time. (3) The alternative effects of $f_{AY}\Delta t_A = -f_{BY}\Delta t_B$ (see Fig. 4) due to $l_{AY} + l_{BY} = -1$ in Eq. 6 would cause a periodic oscillation. (4) Oscillatory reactions are usually accompanied by spatio-temporal pattern formation. During $\Delta t_A$ and $\Delta t_B$, A and/or B species are expected to diffuse over catalysts. If the distance is $z$, then $t_L$ may be translated to the spatial period $z_L$ ($=z(t_L)$) of the spatio-temporal patterns.

## Discussion

**Evidence for the Reaction Mechanism.** The three elementary steps, I, II, and III, correspond to the fundamental processes of adsorption, surface reaction, and desorption, respectively. Therefore, it may be regarded as a basic model for a catalyzed reaction of gases. On the other hand, the two intermediates, A and B, are supported by spatially resolved techniques as follows: (1) Surface reconstruction model suggesting two kinds of intermediates is a generally accepted explanation for the complex behavior of CO oxidation on platinum:[4] (a) fcc bulk structure $(1 \times 1) \rightarrow$ "missing-row" $(1 \times 2)$ on Pt(110) and (b) bulk-like $(1 \times 1) \rightarrow$ quasi-hexagonal (hex) on Pt(100). The two different intermediates, $A_X$ and $B_X$ and $A_Y$ and $B_Y$, could be attributed to the two kinds of surface.

From an in situ X-ray diffraction experiment, a periodic oxidation and reduction of Pt metals takes place during rate oscillations in catalytic CO oxidation on a supported Pt catalysts.[16] Periodic changes in CO-covered $1 \times 1$–c$(2 \times 2)$ phase and reconstructed hex phase on Pt(100) have been demonstrated by in situ LEED measurements.[18] It has been shown further in CO oxidation on Pt(110) that the presence of the gas phase at high pressures of ca. 100 Pa can stabilities surface structures by using scanning tunneling microscopy inside a high-pressure flow reactor and there is a strict one-to-one correspondence between the surface structure and the catalytic activity.[19]

(2) $A_X$ and $B_X$ species may be assigned to the linearly adsorbed CO species on $Pt/Al_2O_3$ observed by FT-IR.[20] $A_Y$ and $B_Y$ may be regarded as the chemisorbed oxygen and subsurface oxygen, respectively.[21] It has been shown on Pt(100) that the conversion of chemisorbed oxygen to subsur-

face oxygen starts from the interface between hex and $1 \times 1$ surfaces and proceeds toward the interior of the island as a wave; the entire chemisorbed oxygen island has converted to subsurface oxygen.[22,23] In addition, the conversion of chemisorbed oxygen to subsurface oxygen is accompanied by the disappearance of the surrounding CO islands, which supports the simultaneous change of $A_X \leftrightarrow B_X$ (at step $II_X$) and $A_Y \leftrightarrow B_Y$ (at step $II_Y$) in Eq. 11;[23] the reverse of $A_Y \leftarrow B_Y$ may be neglected, because the value of $k_{-BY}$ in Table 1 was negligible.

**Relaxation Times of ΔA and ΔB.** The restrictions of Eqs. 10 and 11 lead to

$$(\mu_{AX} - \mu_X) + (\mu_{AY} - \mu_Y) = 0, \tag{61}$$

$$(\mu_{BX} - \mu_{AX}) + (\mu_{BY} - \mu_{AY}) = 0, \tag{62}$$

respectively, which can be rewritten as

$$\mu_{AX} + \mu_{AY} = \mu_X + \mu_Y, \tag{63}$$

$$\mu_{BX} + \mu_{BY} = \mu_{AX} + \mu_{AY}. \tag{64}$$

Since Eqs. 63 and 64 mean local equilibriums at step I and II, the reverse reaction at each step is possible.

The material balance for $B_X$ species, for example, may be expressed by

$$dB_X/dt = S_{IIX} - (S_{-IIX} + R_X) - R_Y, \tag{65}$$

where $S_{IIX}$, for example, denotes the forward reaction rate at step $II_X$. When the steady state is perturbed harmonically, (see Fig. 2)

$$\Delta_\omega dB_X/dt = k_{AX}{}^* \Delta_\omega A_X - (k_{-BX} + k_{BX}{}^*)\Delta_\omega B_X - k_{BY}{}^* \Delta_\omega B_Y, \tag{66}$$

where the subscript $\omega$ is added in order to emphasize the harmonic oscillation.

If $\Delta_\omega S_{IIX}$ and $\Delta_\omega R_Y$ are stopped abruptly at a moment, then the deviation from the steady state at the moment, $\Delta B_X$, would decrease according to the rate equation:

$$\Delta dB_X/dt = -(k_{-BX} + k_{BX})\Delta B_X, \tag{67}$$

where $\omega = 0$ is considered. Equation 67 leads to

$$\Delta B_X(t) = \Delta B_X(0) \exp\{-(k_{-BX} + k_{BX})t\}. \tag{68}$$

The relaxation time of $\Delta B_X(0)$ is given therefore by $(k_{-BX} + k_{BX})^{-1}$.

The results of $k$'s in the course of (i) corresponding to component X were one or two orders of magnitude larger than those in (ii) corresponding to component Y (see Table 1). It was therefore concluded that relaxation time of $\Delta A_X$ and $\Delta B_X$ was on the order of 1 s, while that of $\Delta A_Y$ and $\Delta B_Y$ was on the order of 1 min. It agrees with the fact that only diffusion of adsorbed CO has been considered in a standard kinetic model for the reaction.[4,24,25]

**Flow of Gibbs Free Energy.** (1) The appearance rate of Z was perturbed by $\Delta_\omega P_X(t)$ and $\Delta_\omega P_Y(t)$ in this work. The variation was expressed well by a linear function:[9]

$$\Delta_\omega R(t) = H_X{}^* \Delta_\omega P_X(t) + H_Y{}^* \Delta_\omega P_Y(t), \tag{69}$$

where $H_X{}^*$ and $H_Y{}^*$ represent complex functions involving the sixteen rate coefficients as well as $\omega$.

It was found that contribution of $H_Y{}^* \Delta_\omega P_Y(t)$ to $\Delta_\omega R(t)$ was superior to $H_X{}^* \Delta_\omega P_X(t)$ and phase difference between $\Delta_\omega R(t)$ and $H_X{}^* \Delta_\omega P_X(t)$ was very larger than that between $\Delta_\omega R(t)$ and $H_Y{}^* \Delta_\omega P_Y(t)$.[9] The results are consistent with the facts that the overall free energy dissipations, $x(-\Delta g_T)r_s$, have been attributed to (i) corresponding to species X, whereas the dispersions in the course of (ii) corresponding to species Y cancel out.

(2) Although the reaction mechanism contains many kinetic coefficients, the falls model is characterized by only two parameters, $l_{BX}$ (or $x$) and $\lambda$, provided that $r_s$ is known. It is noted that $t_L$, $r_s$, and $f_T$ in Eqs. 58–60 are characterized by $x$ and $\lambda$ and $x$ is correlated to $l_{BX}$ by Eq. 12. This means that the two parallel transformations, (i) and (ii), are strongly coupled over catalysts, which denies the global coupling through gas phase supposed.[5]

(3) Only $l_{BX}$ among all $l$'s was positive, which means

$$\partial \ln \mu_{BX}/\partial \ln B_X < 0, \tag{70}$$

suggesting that step $III_X$ appears to be a unique step.

(4) Although the impulse at step $III_X$ plays an active role in Eq. 34, the physical meaning is unknown.

**Support for Dissipative Structure.** The system of $X + Y \rightarrow Z$ in a steady state may be regarded as a kind of dissipative structure, because (1) $(-\Delta g_T)$ indicates distance from thermodynamic equilibrium, (2) $y(-\Delta g_T)r_s$ corresponds to momentum produced by consumption of $x(-\Delta g_T)r_s$, (3) the rate oscillation of $t_L$ arises from the destruction of heat balance of $q_+ = q_-$, and (4) surroundings characterized by $\lambda$ are indispensable for the structure to be supported.

It should be emphasized that $f_T$ that supports the structure arises spontaneously from the interaction between catalysts and thermal surroundings, and therefore, an autocatalytic reaction, such as $A + X \leftrightarrow 2X$ postulated,[1] is not required in this kinetic model.

**Application to Other Reactions.** The reaction mechanism is probably oversimplified. However, it may be a basic mechanism in an associative reaction expressed by $X + Y \rightarrow Z$. For instance, a catalyzed hydrogenation of ethene may be divided into two parallel transformations of

(i) $\mathbf{H}_2(X) \leftrightarrow 2\mathbf{H}(A_X) \leftrightarrow \mathbf{H}C_2H_4 \ldots \mathbf{H}(B_X) \rightarrow \mathbf{H}C_2H_4\mathbf{H}(Z_X)$,

and

(ii) $\mathbf{C}_2\mathbf{H}_4(Y) \leftrightarrow \mathbf{C}_2\mathbf{H}_4(A_Y) \leftrightarrow H\mathbf{C}_2\mathbf{H}_4(B_Y) \rightarrow H\mathbf{C}_2\mathbf{H}_4H(Z_Y)$,

so that the falls model would be applicable.

In order to apply RRS to any reaction, the condition

$$|\Delta P_W(\omega)/\Delta P_0(\omega)| - 1 \neq 0 \tag{71}$$

should be satisfied,[9] because deviation from unity is attributed to reaction-rate, where W denotes X, Y, or Z (see Fig. 1a) and 0 is an inert gas added as a reference gas, e.g., Ar in this work.[9] The condition is expected to depend on partial pressure and temperature of the reaction as well as $\omega$.

## Conclusion

The falls model based on $f$ derived from $j(t)$ is effective to describe quantitatively a variety of couplings contained in a CO oxidation that are difficult to be found by spatially resolv-

ing techniques. The RRS based on $-\mathrm{d}G(\tau)/\mathrm{d}t$, instead of $-G(\tau)$ in a TS theory, would be valid to study kinetics of a dissipative structure that is dominant in nature.

Similar data analysis for Ru with $l_{\mathrm{BX}} = 0.501$[9] were possible and similar results to those of Pt reported in this work were derived. However, RRS data for Cu were insufficient to obtain reliable parameters; more accurate investigation is required. Application to a preferential CO oxidation in hydrogen seems to be of interest because of practical importance, and extending the work to a dissociative reaction, such as $\mathrm{Z} \rightarrow \mathrm{X} + \mathrm{Y}$, seems to be of theoretical interest.

The author wish to thank Dr. F. Nemoto (Osaka Institute of Technology) for fruitful discussions about the falls model.

## References

1 G. Nicolis, I. Prigogine, *Self-Organization in Non-equilibrium Systems*, Wiley, New York, **1977**.

2 D. Gurel, O. Gurel, *Oscillations in Chemical Reactions*, Springer-Verlag, Berlin, **1983**.

3 F. Schueth, B. E. Henry, L. D. Schmidt, *Adv. Catal.* **1993**, *39*, 51.

4 R. Imbihl, G. Ertl, *Chem. Rev.* **1995**, *95*, 697.

5 A. v. Oertzen, H. H. Rotermund, A. S. Mikhailov, G. Ertl, *J. Phys. Chem. B* **2000**, *104*, 3155.

6 H. Eyring, *J. Chem. Phys.* **1935**, *3*, 107.

7 M. G. Evans, M. Polanyi, *Trans. Faraday Soc.* **1935**, *31*, 875.

8 a) J. Horiuti, *J. Res. Inst. Catal., Hokkaido Univ.* **1958**, *6*, 250. b) J. Horiuti, K. Miyahara, *NSRDS-NBS 13*, Government Printing Office, Washington. D.C., **1968**.

9 Y. Yasuda, A. Matsumoto, R. Oda, *Bull. Chem. Soc. Jpn.* **2004**, *77*, 1973.

10 For example: M. Bertram, C. Beta, H. H. Rotermund, G. Ertl, *J. Phys. Chem. B* **2003**, *107*, 9610.

11 Y. Yasuda, *Heterog. Chem. Rev.* **1994**, *1*, 103.

12 a) C. A. Becker, J. P. Cowin, L. Wharton, D. J. Auerbach, *J. Chem. Phys.* **1977**, *67*, 3394. b) C. B. Mullins, C. T. Rettner, D. J. Auerbach, *J. Chem. Phys.* **1991**, *95*, 8649. c) T. Matsushima, *Heterog. Chem. Rev.* **1995**, *2*, 51. d) P. K. Stefanov, Y. Ohno, T. Yamanaka, Y. Seimiya, K. Kimura, T. Matsushima, *Surf. Sci.* **1998**, *416*, 305. e) M. G. Moula, S. Wako, G. Cao, K. Kimura, Y. Ohno, I. Kobal, T. Matsushima, *Phys. Chem. Chem. Phys.* **1999**, *1*, 3677.

13 a) D. A. Mantell, S. B. Ryali, G. L. Haller, J. B. Fenn, *Chem. Phys. Lett.* **1981**, *81*, 185. b) D. A. Mantell, S. B. Ryali, G. L. Haller, *Chem. Phys. Lett.* **1983**, *102*, 37. c) D. A. Mantell, K. Kunimori, S. B. Ryali, G. L. Haller, J. B. Fenn, *Surf. Sci.* **1986**, *172*, 281. d) C. Wei, G. L. Haller, *J. Chem. Phys.* **1996**, *105*, 810. e) E. Molinari, M. Tomellini, *Chem. Phys.* **2002**, *277*, 373.

14 W. X. Huang, X. H. Bao, H. H. Rotermund, G. Ertl, *J. Phys. Chem. B* **2002**, *106*, 5645.

15 Strictly, the contribution of $y(-\Delta g_{\mathrm{T}}) = 36.9\,\mathrm{kJ}$ should be subtracted.

16 N. Hartmann, R. Imbihl, W. Vogel, *Catal. Lett.* **1994**, *28*, 373.

17 S. Derrouiche, D. Bianchi, *J. Catal.* **2005**, *230*, 359.

18 R. Imbihl, M. P. Cox, G. Ertl, *J. Chem. Phys.* **1986**, *84*, 3519.

19 B. L. M. Hendriksen, J. W. M. Frenken, *Phys. Rev. Lett.* **2002**, *89*, 046101.

20 a) A. Bourane, D. Bianchi, *J. Catal.* **2001**, *202*, 34. b) A. Bourane, D. Bianchi, *J. Catal.* **2002**, *209*, 114. c) A. Bourane, D. Bianchi, *J. Catal.* **2002**, *209*, 126.

21 a) R. Imbihl, M. Sander, G. Ertl, *Surf. Sci.* **1988**, *204*, L701. b) A. L. Vishnevskii, V. I. Savchenko, *React. Kinet. Catal. Lett.* **1989**, *38*, 187.

22 J. Lauterbach, K. Asakura, H. H. Rotermund, *Surf. Sci.* **1994**, *313*, 52.

23 N. McMillan, T. Lele, C. Snively, J. Lauterbach, *Catal. Today* **2005**, *105*, 244.

24 R. Imbihl, M. P. Cox, G. Ertl, H. Mueller, W. Brenig, *J. Chem. Phys.* **1985**, *83*, 1578.

25 J. Verdasca, P. Borckmans, G. Dewel, *Phys. Chem. Chem. Phys.* **2002**, *4*, 1355.